Effect of Mo and Pd on the grain-boundary cohesion of Fe

W. T. Geng and A. J. Freeman
Department of Physics and Astronomy, Northwestern University, Evanston, Illinois 60208

R. Wu
Department of Physics and Astronomy, California State University, Northridge, California 91330

G. B. Olson
Department of Materials Science and Engineering, Northwestern University, Evanston, Illinois 60208
(Received 21 December 1999; revised manuscript received 6 April 2000)

The effects of Mo and Pd segregation on the cohesion of the Fe $\Sigma 3(111)$ grain boundary are investigated by using the first-principles full-potential linearized augmented-plane-wave total-energy–atomic-force method with the generalized gradient approximation. Based on the Rice-Wang model, our total energy calculations show that Mo has a significant beneficial effect on the Fe grain-boundary cohesion, while Pd behaves as a weak embrittler. An analysis of the geometry optimization indicates that Mo has a moderate atomic size to fit well in the grain-boundary hole, whereas Pd introduces a larger perturbation on the atomic structure near the grain boundary. The elastic energy associated with the Mo and Pd segregation is estimated with a rigid environment approximation. It is found that both Mo and Pd introduce a beneficial volume effect. Studies of the electronic structures show that its strong bonding capability makes Mo a cohesion enhancer (-0.90 eV) for the Fe $\Sigma 3(111)$ grain-boundary. By comparison, its weak bonding capability leads Pd to be a weak embrittler ($+0.08$ eV). Our first-principles quantum-mechanical results support the main idea of the atomistic theories in that the elemental cohesive energy difference between the substitutional element and the host element plays an important role in determining its effect on the grain-boundary cohesion. However, the numerical results for Pd, which has a similar elemental cohesive energy to that of Fe, point to the importance of the role played by the volume effect. It is expected that in a lower-angle Fe grain boundary which has a larger grain-boundary volume expansion, Pd can possibly become a cohesion enhancer.

I. INTRODUCTION

Intergranular embrittlement is often the controlling factor limiting the ductility of high-strength metallic alloys.[1] It has been known for decades that impurities and alloying additions segregated to the grain boundary (GB) can have a significant effect on the GB cohesion of alloy steels.[2,3] Alloy designers, on the one hand, have built various atomistic theories, such as thermodynamic[4–6] and semiempirical pair bonding[7] models, to understand and predict the influence of the segregants on the mechanical properties of the GB. Electronic structure theorists, on the other hand, have employed both empirical[8,9] and first-principles quantum-mechanical methods in their calculations.[10–15] While the atomistic treatments, which contact directly with our chemical intuition, have traditionally served as the starting point for materials design, the quantum-mechanical first-principles investigations, which are physically better founded and numerically more accurate, become more demanding in the theoretical explorations of advanced materials. The dialogue between these two sides is in rapid progress, mainly attributed to recent advances in computational physics and the enormous increase in the power of computers and their easy availability. In spite of the complexity of the mechanical behavior and GB atomic structures, general trends in certain mechanical properties can be correlated with specific features of electronic structure.[16] One good example for addressing such a relationship is the Rice-Wang theory,[17] which shows that the potency of a segregation impurity in reducing the ''Griffith work'' of a brittle boundary separation is a linear function of the difference in binding energies for that impurity at the GB and the free surface. Based on the Rice-Wang model, first-principles investigations have given correct predictions of the effects of several impurities on GB intergranular embrittlement.[13–15]

While extensive experimental research[6,18] has been performed on the strengthening effect of Mo on the Fe GB cohesion, the microscopic cause of the role played by the Mo additions has not been well understood. It is known that the bonding character and atomic size are the key factors in determining the cohesion behavior of the alloying additions. However, a highly precise quantitative understanding of the beneficial effect of Mo on the Fe GB is still not available. Very recently, Sagert *et al.*[14] calculated the elctronic effects of Mo and Pd on the chemical embrittlement of the Fe GB by the embedded molecular cluster variational method within the local density approximation (LDA). Mo was found to be a strong GB cohesion enhancer, in agreement with experiment. Pd, for which there is no experimental information, was also found to be a GB cohesion enhancer. However, since boundary effects in the embedded-cluster variational method are not negligible, the numerical results obtained, therefore, need to be verified. Also, the lack of full geometry optimization further weakens the conclusion drawn from these results.

In the present study, we apply the full-potential linearized

augmented-plane-wave (FLAPW) method[19] with the generalized gradient approximation[20] (GGA) to investigate the influence of Mo and Pd on the Fe $\Sigma 3(111)$ GB cohesion. Full relaxation for both free suface (FS) and GB systems is determined from the calculated atomic forces. Based on the Rice-Wang model, our total energy calculations show that Mo has a significant beneficial effect on Fe GB cohesion, in qualitative agreement with both experiment[6,18] and the embedded-cluster variational method.[14] However, for Pd, the present FLAPW calculations predict it to be a weak embrittler, and so different from that given by the embedded-cluster variational method.[14] An analysis of the atomic structure indicates that Mo has an appropriate atomic size to fit into the GB hole, while the Pd has to displace the surrounding Fe atoms slightly further apart across the GB. A rigid environment approximation is used to evaluate the elastic energy associated with Mo and Pd segregation. In the sense of volume matching only, both Mo and Pd are more favorable than Fe in the Fe $\Sigma 3(111)$ GB. By examination of the electronic structures, we find that it is mainly its bonding capability, compared with Fe, that makes Mo a cohesion enhancer for the Fe $\Sigma 3(111)$ GB, whereas its weak bonding capability leads Pd to be an embrittler.

Our first-principles quantum-mechanical results support the idea of the atomistic[5–7] approach in that the elemental cohesive energy difference between the alloying element and the host element plays an important role in determining the effect of this alloying element on the host GB cohesion. However, our calculations on Pd point to the importance of the role played by the volume effect. Thus, the atomic structure of the GB has to be determined with high accuracy in order to predict the behavior of the segregants near the GB, especially for those which have elemental cohesive energies similar to that of the host element. The rest of the paper is organized as follows. In Sec. II, we present the model and computational details. Size mismatch is discussed in Sec. III. In Sec. IV, we interpret the chemical interactions. The mechanism for the cohesive properties of Mo and Pd at the Fe $\Sigma 3(111)$ GB is discussed in Sec. V, and in Sec. VI, we give a short summary.

II. COMPUTATIONAL DETAILS

As sketched in Fig. 1, both the FS and GB were simulated by a slab model,[21] which minimizes the impurity-impurity interactions inherent in the use of superlattice cells. For the FS systems, the Fe(111) substrate was simulated by an 11-layer slab, and the Mo or Pd adatoms were placed pseudomorphically on the next Fe sites on both sides of this slab. For the GB system, a 23-layer slab was adopted to simulate the clean Fe $\Sigma 3(111)$ GB, and the Mo or Pd adatoms replaced the Fe(1) site in the GB core. With 11 layers of Fe atoms in between, the remaining FS-FS and FS-GB interactions were expected to be sufficiently reduced. As we did in a previous LDA study on the effect of carbon as an impurity on the Fe grain-bounday cohesion,[22] the two-dimensional lattice constant was chosen to be that of the experimental bulk value for bcc Fe, 5.42 a.u., and the unrelaxed (111) interlayer distance is therefore 1.564 a.u. The lattice constant for bcc Fe reproduced by our GGA calculation is 5.38 a.u., i.e., about 1% smaller than the experimental value.

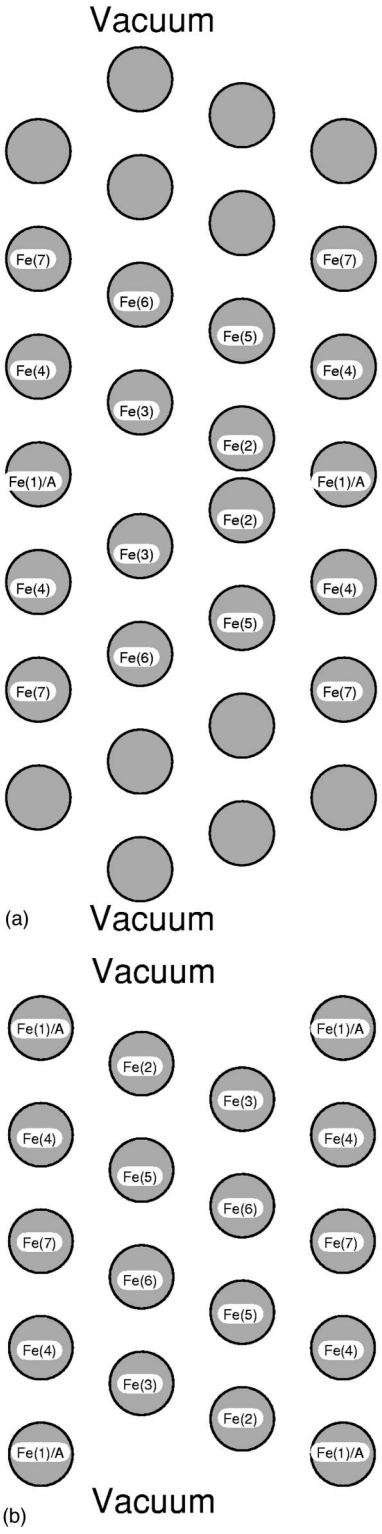

FIG. 1. Model and notation for the structure of Fe and Mo/Pd segregants at (a) the Fe $\Sigma 3(111)$ [001] grain boundary and (b) the Fe(111) free surface.

In the FLAPW method, no shape approximations are made to the charge densities, potentials, and matrix elements. For both iron and impurity atoms, the core states are treated fully relativistically and the valence states are treated semirelativistically (i.e., without spin-orbit coupling). The GGA formulas for the exchange-correlation potential are from Per-

TABLE I. Calculated interlayer distances (a.u.) near the Fe (111) FS. d_{A2} in column 2 denotes the interlayer distance between $A(=\mathrm{Mo,Pd})$, which replaces Fe(1) during segregation, and Fe(2).

	$d_{12}(d_{A2})$	d_{23}	d_{34}	d_{45}	d_{56}	d_{67}	d_{78}	d_{89}	d_{9-10}
Clean (GGA)	1.47	1.25	1.65	1.56	1.44	1.56			
Clean (Expt.[a])	1.30	1.41	1.62	1.52	1.56	1.56			
Clean (LDA[b])	1.40	1.22	1.60	1.51	1.40	1.52			
Mo/Fe	1.48	1.42	1.57	1.61	1.48	1.56			
Pd/Fe	1.80	1.45	1.60	1.56	1.49	1.56			
Clean (GGA[c])	1.49	1.24	1.69	1.56	1.52	1.56	1.57	1.54	1.56

[a]Reference 23.
[b]Reference 22.
[c]19-layer slab.

dew *et al.*[20] An energy cutoff of 13 Ry was employed for the augmented plane-wave basis to describe the wave functions in the interstitial region, and a 140 Ry cutoff was used for the star functions depicting the charge density and potential. Muffin-tin radii for Fe, Mo, and Pd atoms were chosen as 2.1, 2.5, and 2.5 a.u., respectively. Within the muffin-tin spheres, lattice harmonics with angular momentum l up to 8 were adopted.

Convergence was assumed when the average root-mean-square differences between the input and output charge and spin densities are less than 2×10^{-4} e/(a.u.)^3. The equilibrium atomic positions in the vertical direction of both the FS and GB systems, and their corresponding clean reference systems, were determined according to the calculated atomic forces. In order to simulate a bulklike environment for the GB case, we fixed the interlayer distances of the three outermost Fe layers and adjusted them as a whole along with the others around the GB core. Equilibrium-relaxed structures were assumed when the atomic forces on each atom (or the average on the outermost three layers in the GB case) became less than 0.002 Ry/a.u.

The binding energy difference of an impurity in the FS and GB environments is very small. Hence, to obtain reliable values, the FS and GB systems must be treated on an equal footing and the atomic structures of the FS and GB should also be optimized for the cases with and without impurity atoms. Bearing this in mind, we used the same set of numerical parameters in the FLAPW calculations for both the GB and FS; the calculated atomic and electronic structures are given for the fully relaxed systems.

To predict whether an impurity is an embrittler or a cohesion enhancer to a hosting grain boundary, the total energy of five systems must be determined with high precision. These five systems, as mentioned above, are (1) the fully relaxed A ($A=$Mo, Pd) segregated GB, (2) the fully relaxed clean GB, (3) the fully relaxed A adsorbed FS, (4) the fully relaxed clean FS, and (5) a monolayer of A and Fe at the appropriate lattice spacing. Test calculations done before indicate that the numerical error of the binding difference is less than 0.02 eV. As mentioned above, a force of less than 0.002 Ry/a.u. is viewed as zero, which may result in an over- or underestimation of 0.01–0.02 a.u. for the atomic positions. These errors in atomic structure affect the total energy by only 0.02 eV. Thus, taking all of the above into account, the numerical accuracy of the segregant-GB binding energy is within 0.05 eV.

III. ATOMIC STRUCTURE AND VOLUME EFFECT

The equilibrium atomic structure of the GB in metallic materials is of great importance for understanding many of their physical and mechanical properties. Therefore, in a precise first-principles treatment, one has to fully relax the atoms near the GB. As the segregation of an alloying addition to a GB will inevitably relocate the atoms nearby, the atomic structure of the GB with segregants should also be calculated with the same accuracy and under the same set of parameters to minimize numerical errors.

As illustrated in the Rice-Wang model,[17] the influence of a segregant on the GB resistance to brittle fracture correlates its behavior on the GB system with that on the corresponding FS system. However, the issue of volume mismatch only occurs in the GB environment, since on the FS the adatom has more freedom to adjust its position in the vacuum region. The calculated interlayer distances near the clean and Mo/Pd-segregated Fe(111) FS and $\Sigma3(111)$ GB are listed in Tables I and II, respectively.

Also listed in Table I are the experimental[23] and LDA (Ref. 22) values for the clean surface. The oscillatory feature of the interlayer distances given by the GGA is quite similar to that given by the LDA. GGA values are, in general, 2–3 % larger than those of the LDA, mainly due to the fact that the GGA yields a bulk lattice constant larger than the LDA. However, d_{12}, d_{23}, and d_{56} determined by the GGA are quite different from experimental observation, suggesting that the 13-layer slab might not be thick enough to give a reliable atomic structure of the Fe(111) FS. To test the extent of this reliability, we also simulated the clean Fe(111) FS with a 19-layer slab. The optimized interlayer distances for this system are listed as the bottom row in Table I. Clearly, the interlayer distances deep in the slab recover well the bulk values, indicating that the 19-layer slab is surely thick

TABLE II. Calculated interlayer distances (a.u.) near the clean and Mo/Pd-segregated Fe $\Sigma3(111)$ GB. d_{A2} in column 2 denotes the interlayer distance between $A(=\mathrm{Mo,Pd})$, which replaces Fe(1) during segregation, and Fe(2).

	$d_{12}(d_{A2})$	d_{23}	d_{34}	d_{45}	d_{56}	d_{67}
Clean	2.11	1.25	1.60	1.63	1.50	1.59
Mo/Fe	2.17	1.33	1.46	1.66	1.50	1.56
Pd/Fe	2.21	1.25	1.56	1.64	1.48	1.56

enough to simulate the Fe(111) FS. It is interesting to note that from the 13-layer slab to the 19-layer slab, d_{12} and d_{23} undergo a change of only 0.01–0.02 a.u., but are still quite different from the experimental values.[23] With the increase of the slab thickness, d_{56} is largely restored to the bulk value. While the 13-layer slab gives reliable d_{12}–d_{45}, it is not thick enough to give a reliable d_{56}. To clarify the effect of the error in d_{56} on the energetics of the FS system, we calculated the surface energy with these two slabs. To obtain the surface energy E_S for Fe(111), we assume that any layers beyond 11 inserted into the center of the slab may be considered as additional bulk-like layers. Thus, for an n-layer slab, where $n>11$, E_S is given by

$$E_S = -\frac{1}{2}\left[E_{11} - \frac{11}{n-11}(E_n - E_{11})\right], \tag{1}$$

where E_{11}, the total energy of the 11-layer slab, was determined by separate full FLAPW calculations. We find for $n=13$, $E_S=2.83$ eV, and for $n=19$, $E_S=2.80$ eV. The discrepancy of 0.03 eV is of the same order of magnitude as the numerical accuracy of the segregant-GB binding energy (see Sec. II). These rigorous tests show that the FS-FS interaction across the 13-layer slab is negligible and therefore justifies the employment of such a slab in an investigation concerning energetics.

From Table II, it is seen that both Mo and Pd push Fe(i)-Fe(i) pairs ($i=2$, 3, and 4) farther apart across the GB plane. This is in agreement with the experimental fact that both Mo and Pd have a larger bulk nearest-neighbor distance than Fe. According to our first-principles calculations, the presence of Mo pushes Fe(2)-Fe(2) farther apart by 0.12 a.u. ($=2\Delta d_{12}$), Fe(3)-Fe(3) by 0.28 a.u., and Fe(4)-Fe(4) by 0.00 a.u., while for Pd, they are 0.20, 0.20, and 0.12 a.u., respectively. A simple comparison of the A-Fe(4) (A = Mo, Pd) bond length suggests that Pd is larger than Mo in the Fe $\Sigma 3(111)$ GB environment. However, according to experiment, Pd has a smaller atomic volume than Mo does in bulk.

To address the problem of volume mismatch, the atomic size of the segregant and also the size of the GB hole should be well defined. Unfortunately, the geometric size of an atom has no absolute meaning and its definition depends on the physical, chemical, or mechanical problems under consideration.[24] The problem of defining the size of an atom in metallic solid solutions has been discussed in detail by King[25] in the study of substitutional solid solutions and by de Boer *et al.*[26] in the study of energy effects in transition metal alloys. A widely used definition states that the size of an atom B in a BC alloy is the atomic volume of B in its pure elemental form, and it provides a reliable criterion for applying the Hume-Rothery 15% rule.[27] The atomic size of Fe, Mo, and Pd under this definition is 1.00 (Fe is scaled to 1), 1.32, and 1.24, respectively.

Volume expansion is an important property in the atomic structure of the GB. Its contribution to the space available for the substitutional element has a significant influence on the physical and mechanical behavior of this element. Figure 2 shows the relative deviation, obtained from our first-principles calculations on the clean and Mo/Pd-segregated Fe $\Sigma 3(111)$ GB, of the interlayer spacing normal to the GB plane, Δd, as a function of the number of layers away from the boundary plane. For the clean GB (solid circles), the oscillation of Δd is already negligible at the seventh atomic layer away from the boundary plane. A very local measure for the GB expansion is the relative normal displacement ($2\times d_{12}$) of the two nearest atomic planes across the boundary plane. This gauge was adopted, e.g., by Lu *et al.*[15] in Ni_3Al $\Sigma 5(210)$ and by Chen *et al.*[28] in their pure Ni and Al $\Sigma 5(210)$ studies. A nonlocal measure for the GB expansion should be based on the fact that for atomic planes far away from the GB plane, the local lattice constants must be restored to the perfect bulk values. Therefore, the GB volume expansion can be determined by a volume comparision between a slab containing a GB and a slab containing the same number of atomic layers without a GB. This slab should be thick enough to screen the region where layer-layer distances show apparent ($\geqslant 0.05$ a.u.) oscillations.

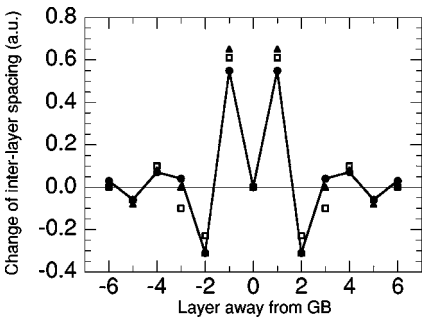

FIG. 2. The calculated relative deviation of the interlayer distances normal to the GB plane. Solid circles, solid triangles, and open squares represent the clean GB, the Pd-segregated GB, and the Mo-segregated GB, respectively.

In the present work, however, our interest is in the local environment surrounding the GB. The GB local environment is determined by Fe(2) together with Fe(3) and Fe(4). The volume of the GB hole, V^{GB}, can therefore be taken as the displacements of Fe(4). The calculated V^{GB} for the Fe $\Sigma 3(111)$ GB is 27.4 a.u.^{3} Only a very small perturbation on the atomic structure of the GB is found for Mo (cf. Fig. 2), meaning that it can fit quite well into the GB when replacing the Fe(1) atom. A slightly larger perturbation occurs when Pd replaces Fe(1), in agreement with the FS case, where our first-principles calculations indicate that Pd is much larger than Mo.

It should be pointed out that not all the expanded volume near the GB is *available* for the GB core atom. As shown below in Sec. V (see Fig. 6), the GB core atom Fe(1) can form bonds only with Fe(4) and Fe(2), but not with Fe(3). This means that only about two-thirds of the GB hole [the left part in Fig. 1(a)] is available for Fe(1). Therefore, the total volume available for the GB core atom is 2/3 of V^{GB} plus V^{Fe}. Now, the volume mismatch ΔV^A between a segregant and the Fe $\Sigma 3(111)$ GB can be defined as

$$\Delta V^A \equiv V^A - \left(V^{Fe} + \frac{2}{3}V^{GB}\right), \tag{2}$$

where A = Fe or any substitutional atom. The calculated ΔV^A for Fe, Mo, and Pd is -18.3, $+7.4$, and $+1.5$, respectively.

TABLE III. Calculated chemical energies (in eV, defined in the text) of Mo, Fe, and Pd in the Fe GB and FS environments.

	Mo	Fe	Pd
$E_{A\text{-}FS}^{chem}$	5.56	4.73	4.11
$E_{A\text{-}GB}^{chem}$	9.17	7.18	6.66
$E_{A\text{-}GB}^{chem}/E_{A\text{-}FS}^{chem}$	1.65	1.52	1.62

To quantify the volume effect of a substitutional addition, one should compare the elastic energy of the clean and segregated GB. This elastic energy is associated with the volume mismatch between the GB core atom and the GB hole. Since the crystal lattice near the GB is not perfect even without the volume mismatch between the GB core atom and the GB hole, the bulk modulus and shear modulus of Fe near the GB no longer retain the perfect bulk values and are not well defined. As a crude approximation, we neglect the relaxation of the GB during segregation and take the effect of the volume mismatch between the GB core atom and the GB hole as only the compression or expansion of the segregant in a rigid environment. The elastic energy associated with the volume mismatch can, therefore, be estimated as

$$E_V^A = \frac{K_A(\Delta V^A)^2}{2V^A}, \tag{3}$$

where ΔV^A is the volume mismatch between the GB core atom and the GB hole. $A=$Fe corresponds to the clean GB case. When Fe(1) is replaced by A, the change of the elastic energy near the GB core, ΔE_V^A, is

$$\Delta E_V^A = E_V^A - E_V^{Fe}, \tag{4}$$

which can be viewed as the volume effect of a substitutional addition A. The calculated ΔE_V^A for Mo and Pd is -0.26 eV and -0.32 eV, respectively. In the sense of volume matching only, Mo and Pd are better matches than Fe in the Fe $\Sigma 3(111)$ GB.

IV. ELECTRONIC STRUCTURE AND BONDING CHARACTERS

The other factor, even more important in general, in determining the behavior of a segregant in the GB is its bonding character in both the GB and FS environments. The calculated chemical energies of the direct interaction between the segregant and the host atoms, defined as the work needed to remove the segregant monolayer to infinity while not permitting the Fe atoms to relax, are listed in Table III. It is clearly seen that Mo has a stronger bonding capability than Fe in both FS and GB situations while Pd is just the opposite, and that all segregants have a stronger chemical interaction in the GB than on the FS.

In real space, the interatomic chemical interaction can be analyzed and understood from the total electronic charge density distribution and the charge transfer between them. Figures 3 and 4 display contour plots of the total charge density in the (110) plane near the Fe FS and $\Sigma 3$ GB, respectively. Figure 1 shows that in the region between Fe(4), Fe(3), Fe(2), and the surface atom, the charge density contours show different features for the adsorbed Mo, Pd FS and the clean FS. The charge density is higher in the case of Mo than the clean surface, and is even lower in the Pd case. This is in keeping with the fact that among these three bulk metals, Mo has the highest interstitial charge density and Pd has the lowest. As a high interstitial charge density generally means strong bonding between atoms, Fig. 3 suggests that Mo has a larger, while Pd has a smaller, binding energy than Fe has at the Fe (111) FS.

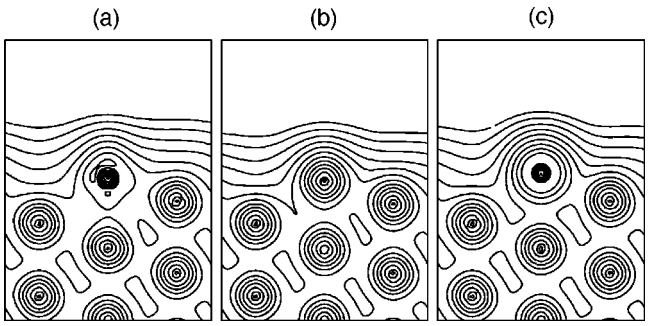

FIG. 3. The calculated total valence charge density for (a) the Mo-adsorbed Fe (111) FS, (b) the clean FS, and (c) the Pd-adsorbed FS. Lines start from 1.25×10^{-3} and increase successively by a factor of 2.

Figure 4 demonstrates that in these three GB systems, Fe(6) has a very similar electronic charge density environment to Fe(7), indicating that the effect of the GB is limited to within six atomic layers away from the GB plane. (The calculated density of states, not shown, also supports this conclusion.) The charge density around the Fe(1) atom is apparently lower than in the bulk region, pointing to an energy loss due to the formation of the GB. When Fe(1) is replaced by Mo, the charge density in the GB core is significantly increased, to a level even higher than the bulk value of Fe. This suggests a stronger Mo-GB interaction than does Fe-GB, i.e., comparable to the FS situation. Nonetheless, the charge density around the Pd atom shows a different character in the GB environment than in the FS. In the GB core, the segregation of Pd also increases the interstitial charge density, making it close to the bulk Fe value. Since Pd has a larger atomic core (taken as the region surrounded by the outermost closed charge density contour centered at the Pd nucleus), the volume of the interstitial region in the GB core

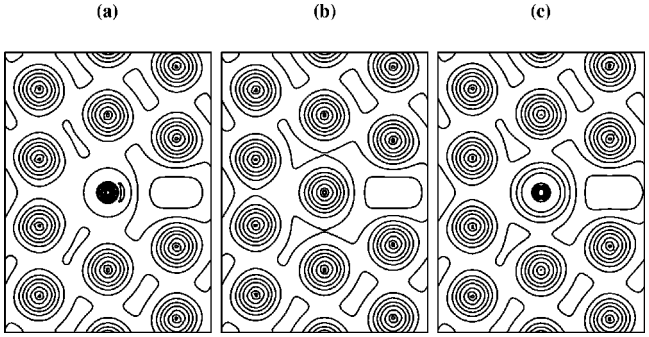

FIG. 4. The calculated total valence charge density for (a) the Mo-segregated Fe $\Sigma 3(111)$ GB, (b) the clean GB, and (c) the Pd-segregated GB. Lines start from 20×10^{-3} and increase successively by a factor of 2.

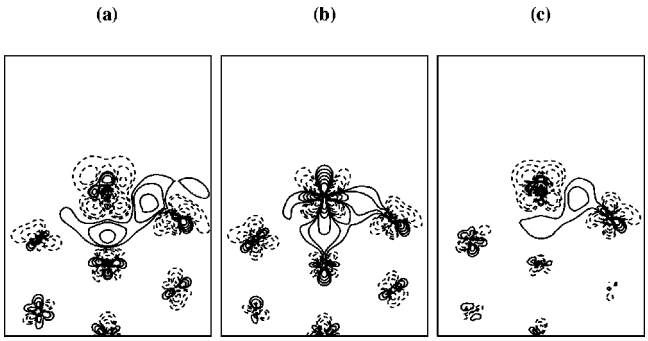

FIG. 5. The calculated valence charge density transfer for (a) the Mo-adsorbed Fe (111) FS, (b) the clean FS, and (c) the Pd-adsorbed FS. Contours start from $5\times10^{-3}e$/a.u.^{3} and increase successively by a factor of 2. Dashed lines denote spin depletion; solid lines denote spin accumulation.

is therefore diminished with Pd segregation. With a higher charge density in a shrunken bonding space, it is not easy to compare the bonding strength of Pd-GB with Fe-GB.

Charge transfer contour plots represent another powerful tool to analyze the interatomic chemical bonding. They contain information because the formation, dissolution, strengthening, and weakening of chemical bonds are always accompanied and characterized by charge accumulation and depletion. This tool is more quantitative because the amount of the interatomic charge transfer during chemical bonding is a small quantity compared with the number of total valence electrons involved. Therefore, from charge transfer, the strengths of different bonds become easier to compare. In Figs. 5 and 6, the calculated charge transfer, obtained by subtracting the superimposed charge density of a free A monolayer (A=Mo, Fe, or Pd) and the clean Fe reference slab from the charge density of the corresponding A/Fe system are presented for A/Fe FS and A/Fe GBs, respectively. In both situations, significant charge accumulations are found in the region between Mo [or Fe(1) and Pd] and its nearest-neighbor Fe(2) and Fe(4) atoms, demonstrating significant hybridization between their electronic states. From Fig. 6, a more significant charge accumulation in the GB core region is found for Fe compared with Pd, indicating that the bonding strength of Pd-GB is smaller than that of Fe-GB.

A detailed comparison between Figs. 5 and 6 points out

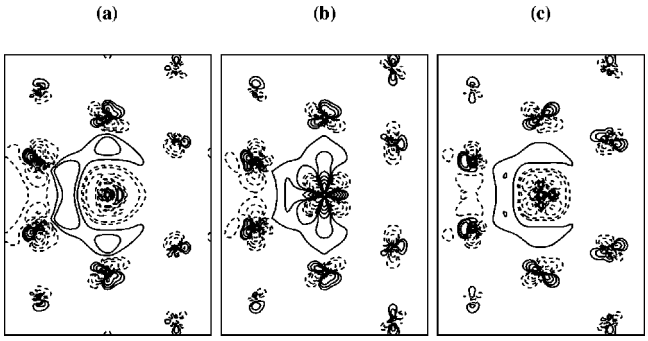

FIG. 6. The calculated valence charge density difference for (a) the Mo-segregated Fe $\Sigma3(111)$ GB, (b) the clean GB, and (c) the Pd-segregated GB. Contours start from $5\times10^{-3}e$/a.u.^{3} and increase successively by a factor of 2. Dashed lines denote spin depletion; solid lines denote spin accumulation.

TABLE IV. Calculated binding energy differences (in eV) between Fe and Mo, Fe and Pd in the Fe GB and FS environments [cf. Eqs. (3) and (4)].

	$\delta\Delta E_s^A$	$\delta\Delta E_b^A$	ΔE_B^A
Mo	−0.95	−1.85	−0.90
Pd	0.65	0.73	0.08

that for these three elements, the charge accumulation in the GB region is apparently stronger than that in the FS case, as the coordination number doubles from the FS to the GB. This can be explained semiempirically by the $\sqrt{Z}$ theory.[29,30] The simplest expression of band character is in the second-moment approximation to the tight-binding model, in which the cohesive energy per atom (with fixed bond length) varies as $\sqrt{Z}$, where Z is the atomic coordination which can range from 1 (diatomic molecule) to 12 (fcc crystal). For the segregant in the Fe $\Sigma3(111)$ GB, $Z=8$, and for that on the Fe (111) FS, $Z=4$. So by applying the $\sqrt{Z}$ rule one will get

$$E_{A\text{-}GB}^{chem}=\sqrt{2}\times E_{A\text{-}FS}^{chem}.$$

The calculated $E_{A\text{-}GB}^{chem}/E_{A\text{-}FS}^{chem}$ for Fe, Mo, and Pd is 1.65, 1.52, and 1.62, respectively (see Table III). We should point out that the $E_{A\text{-}GB}^{chem}$ and $E_{A\text{-}FS}^{chem}$ are those from the relaxed systems and have different bond lengths; therefore they are not strictly comparable with the $\sqrt{2}$ value. However, the similarity of the values of $E_{A\text{-}GB}^{chem}/E_{A\text{-}FS}^{chem}$ does imply that the contribution of chemical bonding to the strengthening-embrittling effect of a segregant is roughly proportional to the difference between its cohesive energy and that of Fe.

V. COMBINED EFFECT AND CONCLUSION

As stated above, in the Rice-Wang theory,[17] the potency of a segregant in reducing the ''Griffith work'' of a brittle boundary separation is a linear function of the difference in binding energies (ΔE_B) for that segregant at the grain boundary (ΔE_b) and the free surface (ΔE_s). If this segregant occupies a substitutional position, i.e., replaces a host atom in the GB core [Fe(1) in this work], its embrittlement potency is then determined by the difference in binding energy differences

$$\Delta E_B=\delta\Delta E_b-\delta\Delta E_s, \tag{5}$$

where

$$\delta\Delta E_b=\Delta E_b^A-\Delta E_b^{Fe}, \quad \delta\Delta E_b=\Delta E_b^A-\Delta E_b^{Fe},$$
$$A=\text{Mo, Pd}. \tag{6}$$

The calculated $\delta\Delta E_s$, $\delta\Delta E_b$, and ΔE_B for Mo and Pd are are listed in Table IV. Mo has an embrittlement potency of −0.90 eV. This means that when segregated to the Fe $\Sigma3(111)$ GB, Mo acts as a strong cohesion enhancer. By contrast, for Pd, ΔE_B is +0.08 eV, and hence it is a weak embrittler.

Note that the cohesive energy for bulk Mo, Fe, and Pd is −6.82 eV, −4.29 eV, and −3.94 eV, respectively.[31] At this point, our first-principles calculations support the idea of

the atomistic theory[5–7] in that the elemental cohesive energy difference between the substitutional element and the host element plays an important role in determining the behavior of this substitutional element on the host grain-boundary cohesion. This is because, in general, the chemical bonding character plays the dominant role in the determination of the mechanical behavior of a segregant near the GB and the chemical bonding energies of a segregant near the FS and GB are approximately proportional to its coordination number. We argue, however, that the significance of the first-principles electronic structure treatment lies not only in the fact that it is more accurate than the atomistic theory in describing the local chemical interactions near the FS and GB, but more importantly, also in the fact that it can automatically, through atomic relaxation, take the GB volume expansion into account with high precision. The importance of the first-principles electronic structure treatment becomes critical when the segregant (like Pd) has a similar elemental cohesive energy to that of Fe, and hence the volume effect must be taken into account with high accuracy.

VI. SUMMARY

In conclusion, we have studied the embrittling-strengthening effect of Mo and Pd on the cohesion of Fe $\Sigma 3(111)$ GB employing first-principles total-energy–atomic-force electronic structure theory. Mo is found to be a strong cohesion enhancer (-0.90 eV) and Pd behaves as a weak embrittler ($+0.08$ eV). An atomic structure analysis shows no significant size mismatch between these segregants and the GB hole. The examination of the total valence charge density and charge transfer indicates that its strong bonding capability, compared with Fe, makes Mo a cohesion enhancer. By comparison, its weak bonding capability leads Pd to be an embrittler. Our first-principles results support the main idea of the atomistic theory[5–7] in that the elemental cohesive energy difference between the substitutional element and the host element plays an important role in determining the effect of this substitutional element on the host grain boundary cohesion. Nevertheless, the numerical results for Pd point to the importance of the role played by the volume mismatch, suggesting that in a lower-angle Fe GB which has a larger volume available for the GB core atom, Pd can possibly turn into a GB cohesion enhancer.

ACKNOWLEDGMENTS

This work was supported by the Office of Naval Research (Grant No. N00014-94-1-0188), by a grant of Cray-T90 computer time at the NSF supported San Diego Supercomputing Center, and by a grant of Cray-J90 computer time at the DOD supported Arctic Region Supercomputing Center.

[1] See, e.g., C. L. Briant, and S. K. Banerji, in *Embrittlement of Engineering Alloys*, edited by C. L. Briant and S. K. Banerji (Academic Press, New York, 1983), p. 21.
[2] R. H. Greaves, J. Iron Steel Inst., London **100**, 329 (1919).
[3] R. H. Greaves and J. A. Jones, J. Iron Steel Inst., London **111**, 231 (1925).
[4] R. H. Doremus, J. Appl. Phys. **47**, 1833 (1976).
[5] J. P. Stark and H. L. Marcus, Metall. Trans. A **8**, 1423 (1977).
[6] D. Y. Lee, E. V. Barrera, J. P. Stark, and H. L. Marcus, Metall. Trans. A **15**, 1415 (1984).
[7] M. P. Seah, Acta Metall. **28**, 955 (1979).
[8] M. S. Daw and M. I. Baskes, Phys. Rev. Lett. **50**, 1285 (1983).
[9] T. McMullan, M. J. Scott, and E. Zaremba, Phys. Rev. B **35**, 1076 (1987).
[10] G. S. Painter and F. W. Averill, Phys. Rev. Lett. **58**, 234 (1987).
[11] M. E. Eberhart and D. D. Vvedensky, Phys. Rev. Lett. **58**, 61 (1987).
[12] D. A. Muller, S. Subramanian, P. E. Batson, S. L. Sass, and J. Silcox, Phys. Rev. Lett. **75**, 4744 (1995).
[13] R. Wu, A. J. Freeman, and G. B. Olson, Science **265**, 376 (1994).
[14] L. P. Sagert, G. B. Olson, and D. E. Ellis, Philos. Mag. B **77**, 871 (1997); L. P. Sagert, Ph.D. thesis, Northwestern University, 1995.
[15] G. Lu, N. Kioussis, R. Wu, and M. Ciftan, Phys. Rev. B **59**, 891 (1999).
[16] G. B. Olson, Science **277**, 1237 (1997).
[17] J. R. Rice and J. S. Wang, Mater. Sci. Eng., A **107**, 23 (1989).
[18] C. J. Macmahon, A. K. Cianelli, and H. C. Feng, Metall. Trans. A **8**, 1055 (1977).
[19] E. Wimmer, H. Krakauer, M. Weinert, and A. J. Freeman, Phys. Rev. B **24**, 864 (1981) and references therein; M. Weinert, E. Wimmer, and A. J. Freeman, *ibid.* **26**, 4571 (1982).
[20] J. P. Perdew, K. Burke, and M. Ernzerhof, Phys. Rev. Lett. **77**, 3865 (1996).
[21] R. Wu, A. J. Freeman, and G. B. Olson, J. Mater. Res. **7**, 2403 (1992); G. L. Krasko and G. B. Olson, Solid State Commun. **76**, 247 (1990).
[22] R. Wu, A. J. Freeman, and G. B. Olson, Phys. Rev. B **53**, 7504 (1996).
[23] J. Sokolov, F. Jona, and P. M. Marcus, Phys. Rev. B **33**, 1397 (1986).
[24] W. B. Pearson, *The Crystal Chemistry and Physics of Metals and Alloys* (Wiley, New York, 1972).
[25] H. W. King, *Alloying Behavior and Effects in Concentrated Solid Solutions* (Gordon and Breach, New York, 1966).
[26] F. R. de Boer, R. Boom, W. C. M. Mattens, A. R. Miedema, and A. K. Niessen, *Cohesion in Metals* (North-Holland, New York, 1988).
[27] W. Hume-Rothery, Acta Metall. **14**, 17 (1966).
[28] S. P. Chen, A. F. Voter, R. C. Albers, A. M. Boring, and P. J. Hay, J. Mater. Res. **5**, 955 (1990).
[29] G. Allan, in *Handbook of Surfaces and Interfaces*, edited by L. Dobrzynski (Garland SPTM, New York, 1978), and references therein.
[30] D. Spanjaard and M. C. Desjonqueres, Phys. Rev. B **30**, 4822 (1984).
[31] C. Kittel, *Introduction to Solid State Physics*, 5th ed. (Wiley, New York, 1976).